International Journal of Earth, Energy and Environmental Sciences
ISSN: 2517-942X
Vol:9, No:6, 2015

Production and Characterization of Sol-Enhanced Zn-Ni-Al_2O_3 Nanocomposite Coating

Soroor Ghaziof, Wei Gao

***Abstract*—**Sol-enhanced Zn-Ni-Al_2O_3 nanocomposite coatings were electroplated on mild steel by our newly developed sol-enhanced electroplating method. In this method, transparent Al_2O_3 sol was added into the acidic Zn-Ni bath to produced Zn-Ni-Al_2O_3nano-composite coatings. The chemical composition, microstructure and mechanical properties of the composite and alloy coatings deposited at two different agitation speed were investigated. The structure of all coatings was single γ-Ni_5Zn_{21} phase. The composite coatings possess refined crystals with higher microhardness compared to Zn-Ni alloy coatings. The wear resistance of Zn-Ni coatings was improved significantly by incorporation of alumina nano particles into the coatings. Higher agitation speed provided more uniform coatings with smaller grain sized and slightly higher microhardness. Considering composite coatings, high agitation speeds may facilitate co-deposition of alumina in the coatings.

***Keywords*—**Microhardness, Sol-enhanced electro plating, Wear resistance, Zn-Ni-Al_2O_3 composite coatings.

I. Introduction

IT is known that composite coatings produced by dispersing nano-sized particles in a coating matrix provide better mechanical properties and corrosion resistance [1]. Nanoparticles such as Al_2O_3, TiO_2 and ZrO_2 have been co-deposited with different metal and alloy coatings to produce composite coatings. This traditional process is using electrochemical deposition with nano-sized solid powder mixture into the electrolyte solution. The incorporation content and uniform dispersion of nanoparticles in the deposit are important factors that determine the properties and performance of the composite coatings. However, it is difficult to achieve good particle dispersion especially when they are in the nanometer scale due to very large surface area and surface energy. The nanoparticles tend to agglomerate together and deteriorate the desired properties [2], [3].

In recent years, Zn-Ni alloys have attracted much attention because of their higher corrosion resistance and better mechanical characteristics than pure Zn and other Zn based alloy coatings for steel components [4], [5]. However, demands for Zn-Ni coatings with better mechanical and corrosion properties are increasing for industrial applications. In order to meet the demands from industry, Zn-Ni based composite coatings have recently been developed to improve the mechanical and chemical properties [6], [7].

The current research applies a newly developed sol-enhanced method to prepare Zn-Ni-Al_2O_3 nanocomposite coatings. This method can avoid particle agglomeration by using solution mixing instead of adding solid powders, leading to true dispersed nanoparticle distribution [8], [9]. The technique combines sol-gel methods and traditional electroplating to prepare highly dispersed uniform oxide nanoparticle reinforced metal coatings. Based on this method, when a small amount of transparent sol was added into the electroplating solution, nanoparticles formed in-situ in the electrolyte and co-deposited into the coating matrix [10].

In the present work, attempts were made to produce Zn-Ni-Al_2O_3 composite coatings using a sol enhanced electrodeposition method. Microstructure and mechanical properties of Zn-Ni-Al_2O_3 coatings were studied and compared to Zn-Ni alloy coating. Effect of agitation speed on properties of coatings was also investigated.

II. Materials and Experiments

A. Coatings and Sol Preparation

An acidic sulphate bath was used for electroplating Zn-Ni and Zn-Ni-Al_2O_3 coatings. The composition and electroplating parameters are summarized in Table I. All solutions were prepared with analytical grade reagents and distilled water. The pH of the bath was adjusted to 2 using a dilute H_2SO_4 solution. Mild steel sheet 1 mm in thickness was cut into 25 mm×25 mm pieces and was used as the substrate. Nickel plates on both sides of the electroplating cell were used as anodes. Samples were prepared for coating by mechanically grounding with 600-grit SiC paper; followed by electro polishing in a solution of 95 vol.% acetic acid and 5 vol.% perchloric acid at 20 V for 3 min; and finally washing with distilled water.

For preparing the Al_2O_3 sol, 97% Al tri-sec-butoxide (ATSB) and distilled water were used in the mol ratio of 0.01:12.4. A small amount of absolute ethanol was added into the beaker to dissolve the ATSB. Under magnetic stirring, deionized water was slowly added into the mixture of ATSB and ethanol. Then 30% nitric acid was added into the solution to adjust the pH value to 3.5 and peptize the solution. At this stage, the solution contained white precipitates. This solution was stirred at 60°C until all white precipitates dissolved and clear sol was produced. The average size of the Al_2O_3 particles suspended in alumina sol used in the experiment as reinforcing phase is 10 nm which was measured with Malvern Zetasizer Nano Series Nano-ZS model instrument.

S. Ghaziof is PhD Candidate at Department of Chemical and Materials Engineering, The University of Auckland, P.B 92019, Auckland 1142, New Zealand (corresponding author: phone No. +6493737599-ext. 88667e-mail: sgha108@aucklanduni.ac.nz).

W. Gao is Professor at Department of Chemical and Materials Engineering, The University of Auckland, P.B 92019, Auckland 1142, New Zealand (e-mail: w.gao@auckland.ac.nz).

B. Coating Characterization

The coating morphologies were analyzed using a field-emission scanning electron microscope (FESEM). A MiniPal 2 PW4025 X-ray fluorescence spectrometer (XRF) with Rhodium tube and spinner was also used for composition analysis. LA-ICP-MS test was applied to detect and measure the intensity of aluminum in composite coatings. The phase structure of the coatings was determined by using X-ray diffraction (XRD, D2 Phaser, Bruker AXS, Germany) with Cu Kα radiation (U = 30 kV, I = 10 mA). Diffraction patterns were recorded in the 2θ ranging from 20 to 90° at a step size of 0.02° s^{-1} and a scanning speed of 0.1 s $step^{-1}$. Micro hardness of coatings was measured using a load of 100 g with a holding time of 15 s with a Vickers Hardness Tester. A NANOVEA Tribometer was used to carry out linear reciprocating wear testing. A zirconia ball with diameter of 6 mm was used as the abrasive ball; and the test was carried out at 0.5 N load for 5 min at 100 rpm at room temperature with relative humidity of ~50%. No lubrication was used during the wear tests.

TABLE I
THE COMPOSITION OF ELECTROPLATING BATH AND PROCESSING PARAMETERS

Bath composition and processing parameters	Quantity
$ZnSO_4.7H_2O$	35 $g.L^{-1}$
$NiSO_4.6H_2O$	35 $g.L^{-1}$
$NaSO_4$	80 $g.L^{-1}$
Al_2O_3 sol (for composite coating)	6 $mL.L^{-1}$
Time	10 min
Current density	80 $mA.cm^{-2}$
Agitation speed	600 and1200 rpm

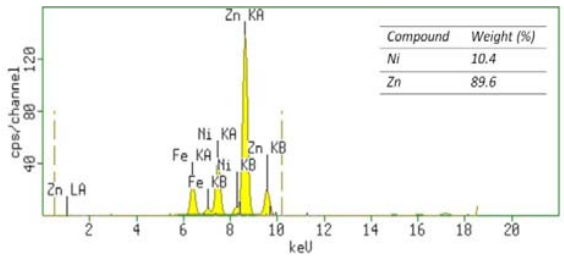

Fig. 1 XRF result for Zn-Ni coating. Electrodeposition parameters: temperature: 40°C, agitation speed: 600 rpm, current density: 80 mA/cm^2, time: 10 min

III. RESULTS AND DISCUSSION

A. Chemical Composition

Zn-Ni alloy coating and Zn-Ni-Al_2O_3 composite coatings were deposited on mild steel at two different agitation speeds, 600 and 1200 rpm. The XRF results of coatings are summarized in Table II. All chemical composition values are quoted in weight percentage, representing the average of at least three measurements. Fig. 2 shows one of the XRF results as a sample. Fe peaks came from the steel substrate.

Results showed that the Ni content of Zn-Ni-Al_2O_3 composite coatings is slightly lower than that Zn-Ni for both agitation speeds. It means that incorporation of alumina into the Zn-Ni coating slightly decreased the Ni content in the coatings. Same results have been observed for Zn-Ni-TiO_2 and Zn-Ni-SiC composite coatings by co-deposition of TiO_2 and SiC particles [11]-[13]. This could be related to the promotion of hydrogen evolution reaction by composite particles on the Zn rich Zn-Ni electrodeposited films, favoring the formation of zinc hydroxide film on the electrode surface that hinders Ni^{2+} reduction [13]. The results also showed that increasing agitation speed slightly decreased the Ni content of both Zn-Ni alloy and Zn-Ni-Al_2O_3 composite coatings which implies that the deposition of Zn was facilitated more by the electrolyte rotation than that of Ni. According to literatures [14], this behavior could be due to the change of chemistry on cathode surface under the combination of high current density and high agitation speed.

TABLE II
XRF AND MICROHARDNESS TEST RESULTS OF ZN-NI COATING ZN-NI-AL2O3 COMPOSITE COATINGS AT TWO DIFFERENT AGITATION SPEEDS

coating	Agitation Speed (rpm)	Ni Content (wt%)	Microhardness (Hv_{100})
Zn-Ni	600[1]	10.5 ± 0.1	208± 6
	1200	10.4 ± 0.1	237± 7
Zn-Ni-Al_2O_3	600	10.2 ± 0.1	293± 12
	1200	10.0 ± 0.1	312± 13

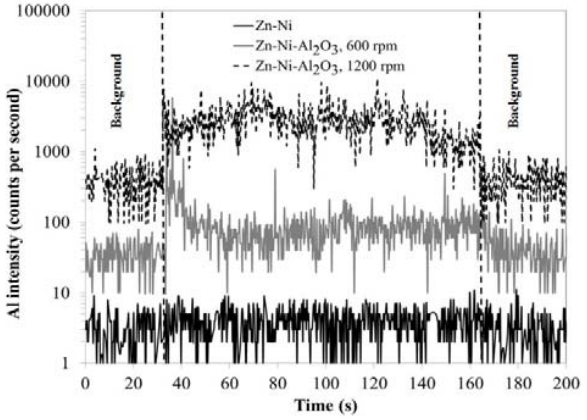

Fig. 2 LA-ICP-MS results of Al for Zn-Ni-Al_2O_3 coatings deposited at two agitation speeds. Analysis from Zn-Ni alloy is also shown for comparison

It is worth mentioning that no Al peak was detected in XRF analysis of composite coatings. This was probably due to the extremely small particle size and relatively low oxide content, being below the detection limit of XRF. However, the results from LA-ICP-MS test on Zn-Ni-Al_2O_3 coatings showed the existence of Al compounds in the coatings. Fig. 2 shows the LA-ICP-MS test results of Al for Zn-Ni-Al_2O_3 composite coatings deposited at different agitation speed and also one Zn-Ni alloy coating without alumina for comparison. These LA-ICP-MS test results provide semi-quantitative results, indicating incorporation of alumina in the coatings. However, it was clear that no Al was detected for the pure Zn-Ni alloy.

In addition, in our previous studies the existence of Al_2O_3nano particles embedded in the Zn-Ni matrix was

confirmed by TEM results and the diffraction pattern for composite coatings [15]

By comparison, however, it can be seen that the Al intensity is almost three times higher for composite coatings deposited at higher agitation speed. Therefore, it seems that the incorporation of alumina into the coatings might be increased by applying higher agitation speed. The reason could be explained by the proposed mechanism of electro deposition of metallic coatings containing nanosized particles by [16]. Based on this theory, the mechanism involves three steps: (1) forced convective of particles to surface; (2) loose adsorption on the surface; (3) irreversible incorporation of particles by reduction of adsorbed ions. Therefore, it could be explained that higher agitation speed during electro deposition could probably facilitate convection of particles to the cathode surface, provide more particles at the cathode surface during the deposition; and as a result this may increase the co-deposition of particles.

B. Phase structure

Fig. 3 shows the XRD pattern of Zn-Ni alloy and Zn-Ni-Al_2O_3 composite coatings at two different agitation speeds. It can be seen that the phase structure of all of deposits is single γ-Ni_5Zn_{21} phase which is the desirable phase structure for Zn-Ni coatings. It has been reported that Zn-Ni coatings of single γ-Ni_5Zn_{21} phase structure with Ni content in the range of 10-14 wt.% has shown five times better corrosion resistant compared to pure Zn [4], [5].

Grain size measurement was conducted based on the Scherrer line broadening equation, which is well suited to detect grain size smaller than 100 nm, and have been used widely for Zn-Ni deposits [5], [17]. The grain size, D, was calculated from broadening of the most intensive peak (330) using the Scherrer equation, $D = 0.9\,\lambda/\beta\cos\theta$, where λ is the wavelength of the radiation (0.154 nm), β is the full width at half-maximum (FWHM) of the peak, and θ is the position of the peak. At 600 rpm, the grain size of Zn-Ni and Zn-Ni-Al_2O_3 coatings were 32±0.4 and 28±0.2 nm, respectively, indicating that the composite coatings have slightly smaller grain size than alloy coatings. Therefore, incorporation of Al_2O_3 nano-particles in the coating refined the crystals.

Results also showed that at higher agitation speed, grain refinement was more pronounced and grain size decreased from 30 ± 0.1 nm for Zn-Ni coating to 23± 0.2 nm for Zn-Ni-Al_2O_3 coating. This could be attributed to more alumina particles incorporated into the deposit. The presence of nano particles can provide more nucleation sites and may slow down the growth of metal grains [11].

It should be noted that all coatings' grain sizes are in the nanometer scale, confirming the nanocrystalline structure of Zn-Ni and Zn-Ni-Al_2O_3 composite coatings.

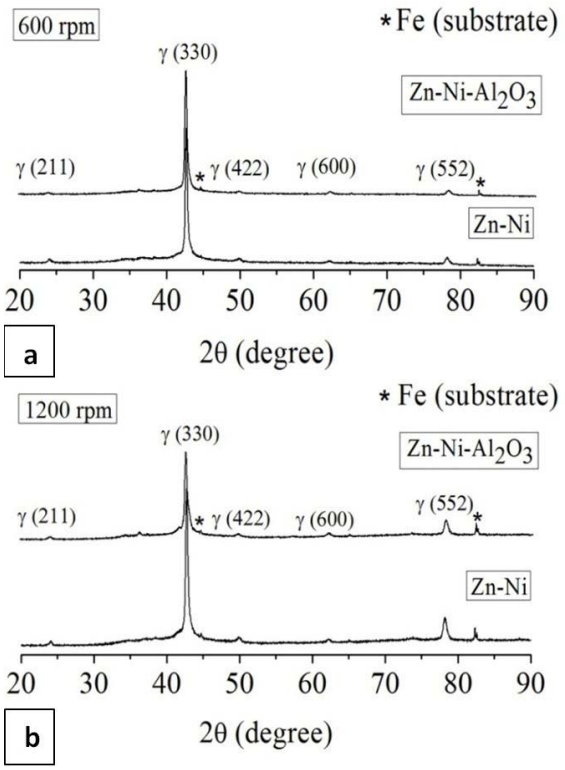

Fig. 3 XRD results for Zn-Ni and Zn-Ni-Al_2O_3 coatings deposited at different agitation speeds (a) 600 rpm, (b) 1200 rpm

C. Surface Morphology

Fig. 4 shows the surface morphology of Zn-Ni and sol enhanced Zn-Ni-Al_2O_3coatings at two different agitation speeds. As can be seen in Figs. 4 (a) and (c), Zn-Ni coatings showed relatively homogeneous hemispherical nodules with average size of 6 μm. However, surface morphology of sol enhanced Zn-Ni-Al_2O_3 composite coatings (Figs. 4 (b), (d)) was completely different from alloy coatings. At 600 rpm agitation speed, composite coating had cauliflower like morphology (Fig. 4 (b)). On the other hand, Zn-Ni-Al_2O_3 coating deposited at higher agitation speed showed smoother nodular background containing some areas with "cauliflower-like" morphology (Fig. 4 (d)). For both alloy and composite coatings, the appearances of coatings were more uniform and the coating color was brighter at 1200 rpm agitation speed compared to 600 rpm.

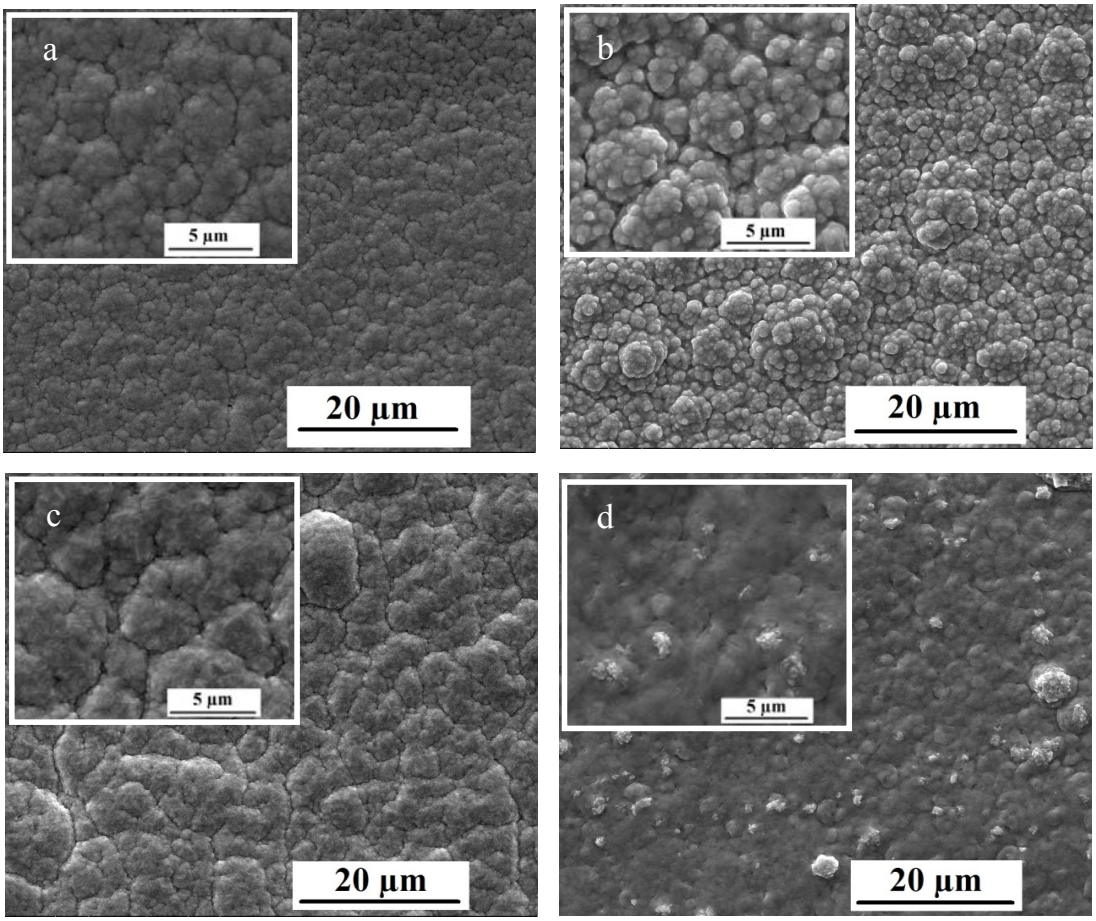

Fig. 4 ESEM images of (a) Zn-Ni coating at 600 rpm, (b) Zn-Ni-Al_2O_3 coating at 600 rpm, (c) Zn-Ni coating at 1200 rpm and (d) Zn-Ni-Al_2O_3 coating at 1200 rpm

D.Mechanical Properties

The micro hardness results of Zn-Ni alloy and Zn-Ni-Al_2O_3composite coatings electroplated at different agitation speeds are summarized in Table II. The results indicated that Zn-Ni-Al_2O_3 composite coatings showed higher micro hardness compared to Zn-Ni alloy coatings. Among all coatings, sol enhanced Zn-Ni-Al_2O_3 composite coating deposited at 1200 rpm had the highest micro hardness (312 ± 13 HV_{100}) and Zn-Ni alloy coating deposited at 600 rpm had the lowest micro hardness (208 ± 6 HV_{100}), a 69% increase. The variation of micro hardness results can be attributed to the incorporation of Al_2O_3nano-particles, Ni content and microstructure changes. As mentioned previously, the Ni content did not change significantly for composite and alloy coatings. Therefore, the increase in micro hardness of the composite coatings should be mainly came from the matrix grain refinement (refer to XRD results) and dispersion strengthening because of incorporation of hard alumina nano particles into the Zn-Ni alloy coating. Dispersion strengthening is associated with the incorporation of fine particles (< 1 µm) and is the result of hindered dislocation motion of matrix by fine particles. In grain refining, the structural refinement is resulted from the nucleation of small grains on the surface of the incorporated particles. The high density of grain boundaries impedes dislocation motion, resulting in increased micro hardness [18].

Comparing the coatings deposited at different agitation speeds, it can be seen that both alloy and composite coatings deposited at 1200 rpm showed slightly higher micro hardness compared to the coatings deposited at 600 rpm (Table II). The reason could be related to higher incorporation of alumina nano particles and smaller grain size as shown by LA-ICP and XRD tests results before. Therefore, based on the micro hardness results and coating appearance, sol enhanced Zn-Ni-Al_2O_3 composite and Zn-Ni alloy coatings deposited at 1200rpm were chosen for more studies.

Wear tests were performed on Zn-Ni alloy and Zn-Ni-Al_2O_3 composite coatings deposited at 1200 rpm. Fig. 5 shows wear track of the coatings. The wear track widths and wear volume loss of the Zn-Ni alloy coating were 292±3 µm and $7\pm0.4\times10^{-3}$ mm^3, respectively. The sol-enhanced Zn-Ni-Al_2O_3 coating showed significantly improved wear resistance, with the narrower wear track width of 225 ± 4 µm and lower wear volume loss of 3 ± 0.4 × 10^{-3} mm^3. Therefore, incorporation of alumina nano particles into the coatings provided composite coatings with better wear resistance.

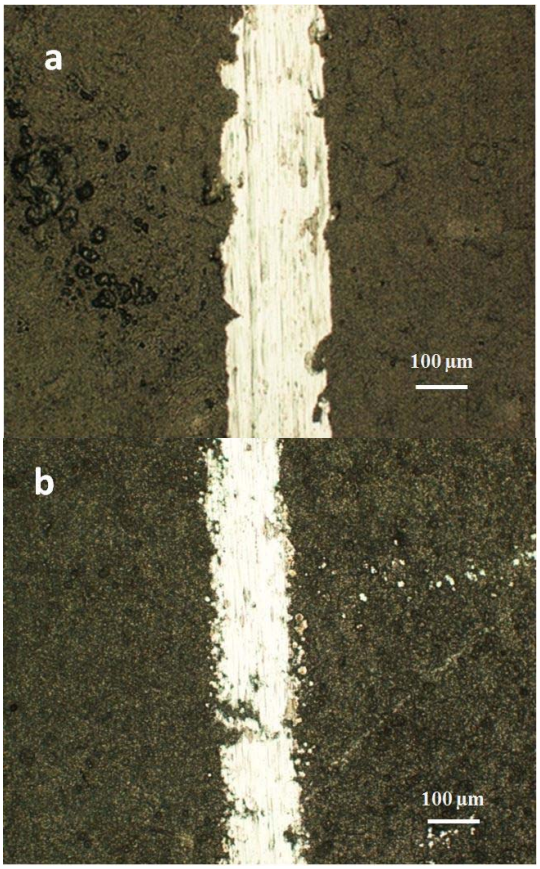

Fig. 5 Wear track of a) Zn-Ni coating and b) Zn-Ni-Al_2O_3 composite coating deposited at 1200 rpm

ACKNOWLEDGMENT

This work is partially supported by a New Zealand Marsden project and NPRP Grant NPRP-4-662-2-249 from the Qatar National Research Fund (a member of Qatar Foundation). The authors would like to thank the technical staff in the Department of Chemical and Materials Engineering, the University of Auckland for their various assistances.

REFERENCES

[1] B.M. Praveen, and T. V. Venkatesha, "Electrodeposition and corrosion resistance properties of Zn-Ni/TiO_2nano composite coatings" Int. J. Electrochem., vol. 2011, pp. 1-4, June 2011.
[2] W. Wang, F. Hou, H. Wang and H. Guo, "Fabrication and characterization of Ni-ZrO_2 composite nano-coatings by pulse electrodeposition" Scr. Mater., vol. 53, pp. 613-618, Sep. 2005.
[3] R. Oberle, M. Scanlon, R. Cammarata, P. Searson, "Processing and hardness of electrodeposited Ni/Al_2O_3 nanocomposites" Appl. Phys. Lett., vol. 66, pp. 19-21, Jan. 1995.
[4] Y. Boonyongmaneerat, S. Saenapitak, K. Saengkiettiyut, "Reverse pulse electrodeposition of Zn-Ni alloys from a chloride bath" J. Alloys Compounds, vol. 487, pp. 479-482, Nov. 2009.
[5] M. M. Abou-Krisha, "Effect of pH and current density on the electro deposition of Zn-Ni-Fe alloys from a sulfate bath" J. Coat. Tech. Res., vol. 9, pp.775-783, 2012.
[6] D. Blejan, D. Bogdan, M. Pop, A.V. Pop and L. M. Muresan, "Structure, morphology and corrosion resistance of Zn-Ni-TiO_2 composite coatings" Optoelectron. Adv. Mater., vol. 5, pp. 25-29, Jan. 2011.
[7] H. Zheng and M. An, "Electrodeposition of Zn-Ni-Al_2O_3nanocomposite coatings under ultrasound conditions" J Alloys Compounds., vol. 459, pp. 548-552, July 2008.
[8] Y. Yang, W. Chen, C. Zhou, H. Xu, W. Gao, "Fabrication and characterization of electroless Ni-P-ZrO_2nano-composite coatings" Appl. Nanosci., vol. 1, pp. 19-26, May 2011.
[9] W. Chen, Y. He, W. Gao, "Electrodeposition of sol-enhanced nanostructured Ni-TiO_2 composite coatings" Surf. Coat. Tech., vol. 204, pp. 2487-2492, Apr. 2010.
[10] W. Chen, Y. He, W. Gao, "Synthesis of nanostructured Ni-TiO_2 composite coatings by sol-enhanced electroplating" J. Electrochem. Soc., vol 157, pp. 122-128, June 2010.
[11] A. Gomes, I. Almeida, T. Frade and A. C. Tavares, "Stability of Zn-Ni-TiO_2 and Zn-TiO_2nanocomposite coatings in near-neutral sulphate solutions" J. Nanoparticle Res., vol. 14, pp. 692-704, Jan. 2012.
[12] A. Gomes, I. Almeida, T. Frade and A. C. Tavares, "Zn-TiO_2 and ZnNi-TiO_2nanocomposite coatings: Corrosion behaviour" Mater. Sci. Forum, vols. 636-637, pp. 1079-1083, Jan (2010).
[13] P. C. Tulio, S. E. B. Rodrigues and I. A. Carlos, "The influence of SiC and Al2O3 micrometric particles on the electrodeposition of ZnNi films and the obtainment of ZnNi-SiC and ZnNi-Al_2O_3electrocomposite coatings from slightly acidic solutions" Surf. Coat. Tech. vol. 202, pp. 91-99, Nov. 2007.
[14] M. R. Kalantary, G. D. Wilcox and D. R. Gabe, "The production of compositionally modulated alloys by simulated high speed electrodeposition from a single solution" Electrochim. Acta., vol. 40, pp. 1609-1616, Aug. 1995.
[15] S. Ghaziof, W. Gao, "The effect of pulse electroplating on Zn-Ni alloy and Zn-Ni-Al2O3 composite coatings" J. Alloys Compounds., vol. 622, pp. 918-924, Feb. 2015.
[16] C. T. J. Low, R. G. A. Wills and F. C. Walsh, "Electrodeposition of composite coatings containing nanoparticles in a metal deposit" Surf. Coat. Tech., vol. 201, pp. 371-383, Sep. 2006.
[17] F. Elkhatabi, M. Benballa, M. Sarret and C. Müller, "Dependence of coating characteristics on deposition potential for electrodeposited Zn-Ni alloys" Electrochim. Acta., vol. 44, pp. 1645-1653, Jan. 1999.
[18] A. Damjanovic, T. Setty, J. Bockris, "Effect of crystal plane on the mechanism and the kinetics of copper electrocrystallization" J. Electrochem. Soc., vol. 113, pp. 429-440, May 1966.